

NOTE

A Higher-Order Godunov Method for the Equations of Ideal Magnetohydrodynamics

1. INTRODUCTION

The last few years have seen the emergence of higher-order extensions of Godunov's method for the solution of general problems in gas dynamics, including a wide variety of astrophysical problems. For example, the PPM algorithm developed by Colella and Woodward [1] has been used to study the stability, evolution, and dissipation of astrophysical jets [2], accretion onto compact objects [3], and the formation of Herbig-Haro objects [4]. PPM is successful in part because it is extremely robust and stable, in part because it is able to resolve shocks and other discontinuities with only a few mesh points, and in part because it is relatively fast. A broad discussion of the philosophy of PPM, along with a comparison between PPM and other numerical methods can be found in Woodward and Colella [5].

However, the structure and dynamics of astrophysical systems are often strongly affected by the magnetic fields which thread them. In particular, the structure and dynamics of galactic jets may be qualitatively different when the effects of magnetic fields are included [6]. As a first step in clarifying the role of magnetic fields in astrophysical jets, and with the hope of duplicating the earlier successes of the PPM code, we have developed a higher-order Godunov method for the equations of ideal magnetohydrodynamics.

A strategy based on a straightforward extension of Godunov's method to MHD quickly runs into two serious difficulties. First, the MHD wave speeds are not strictly hyperbolic. The loss of strict hyperbolicity at a point means that the analytic structure of the weak solutions is in general unknown in the neighborhood of that point. Second, the genuinely nonlinear waves can be locally linearly degenerate. It is much more difficult to determine the correct entropy satisfying discontinuities for modes with local linear degeneracies. To deal with these problems, the starting point for our methodology is a higher-order Godunov method developed by Bell, Colella, and Trangenstein [7] (BCT). We take the point of view in [7] and treat the equations of MHD as a hyperbolic system of conservation laws whose weak solutions are uniquely deter-

mined by entropy conditions such as those described in Liu [8] for such systems. The questions surrounding whether this general approach will produce the correct weak solutions is far from settled; some of these issues are discussed in [7].

The algorithm describe by BCT is an extension of the Engquist-Osher [9] flux to general systems of conservation laws and is sufficiently robust to handle the non-strictly hyperbolic nature of the MHD equations. In the exposition which follows, we rely heavily on BCT for the higher-order solution of the Riemann problem. However, we use a different formulation of the Engquist-Osher flux to deal with both the spatially varying geometry which arises in multi-dimensional simulations and the natural symmetries which arise in the MHD conservation laws. Brio and Wu [10] have also developed a high-resolution method, but their technique requires an adiabatic index $\gamma = 2$ to perform the analytic flux difference splitting.

In Section 2, we develop a complete set of right and left eigenvectors for the one-dimensional projection of the MHD equations. These eigenvectors remain well defined at a point at which the equations are no longer strictly hyperbolic or which at some of the waves become locally linearly degenerate. In Section 3, we describe our extension of the BCT formalism to the equations of ideal MHD, including the alternative formulation of the Engquist-Osher flux. Finally, in Section 4, we present the numerical results for two simple one-dimensional test problems which illustrate some of the complex wave behavior possible in MHD.

2. THE CHARACTERISTICS OF MHD

The BCT algorithm requires both \mathbf{l}_k and \mathbf{r}_k , the left and right eigenvectors of \mathbf{DF} . The standard calculation of \mathbf{r}_k in Jeffery and Tanuti [11] for the one-dimensional version of the MHD equations gives eigenvectors which become indefinite whenever two wave speeds coincide, i.e., at a point at which the system is no longer strictly hyperbolic. Accordingly, we have recomputed a set of \mathbf{r}_k 's in a form which remains well behaved in the neighborhood of a point at which the equations are no longer strictly hyperbolic. In

what follows, we present a derivation of these new eigenvectors normalized so that

$$\mathbf{l}_\alpha \cdot \mathbf{r}_\beta = \delta_{\alpha\beta}.$$

Furthermore, we have assumed that all gradients lie in the x direction and adopted a Cartesian coordinate system with unit vectors \hat{y} and \hat{z} perpendicular to \hat{x} .

The conventional basis for MHD is the Eulerian vector \mathbf{U} , written explicitly as

$$\mathbf{U} = [\rho, \rho u_x, \rho u_y, \rho u_z, B_y, B_z, \rho E]^t,$$

where

$$\rho E = \frac{1}{2} \rho u^2 + \frac{p}{\gamma - 1} + \frac{B_\perp^2}{8\pi} \quad (1)$$

and $\mathbf{B}_\perp = B_y \hat{y} + B_z \hat{z}$. The normal component of the magnetic field, B_x , cannot be advanced in time in a one-dimensional version of MHD. The corresponding flux vector is

$$\mathbf{F}(\mathbf{U}) = \begin{bmatrix} \rho u_x \\ \rho u_x^2 + p + \frac{B_\perp^2}{8\pi} \\ \rho u_x u_y - \frac{B_x B_y}{4\pi} \\ \rho u_x u_z - \frac{B_x B_z}{4\pi} \\ u_x B_y - u_y B_x \\ u_x B_z - u_z B_x \\ \left(\rho E + p + \frac{B_\perp^2}{8\pi} \right) u_x - \frac{B_x}{4\pi} \mathbf{u}_\perp \cdot \mathbf{B}_\perp \end{bmatrix}.$$

Rather than perform a direct calculation of the eigenvectors of $D\mathbf{F}/D\mathbf{U}$, we find it simpler to work in the basis \mathbf{W} , where

$$\mathbf{W} = [\tau, u_x, u_y, u_z, B_y, B_z, p]^t \quad (2)$$

and $\tau = 1/\rho$ is the specific volume. We then construct the eigenvalues and eigenvectors of the matrix

$$\mathbf{A} = \left[\frac{\partial \mathbf{U}}{\partial \mathbf{W}} \right]^{-1} \frac{\partial \mathbf{F}}{\partial \mathbf{W}}. \quad (3)$$

Let \mathbf{R}_A be the matrix whose columns are the right eigenvectors of \mathbf{A} , and let \mathbf{L}_A be the matrix whose rows are the left eigenvectors of \mathbf{A} . Then the right eigenvectors of $D\mathbf{F}/D\mathbf{U}$ are the columns of the matrix

$$\mathbf{R}_U = \frac{\partial \mathbf{U}}{\partial \mathbf{W}} \mathbf{R}_A, \quad (4)$$

while the left eigenvectors are the rows of the matrix

$$\mathbf{L}_U = \mathbf{L}_A \left[\frac{\partial \mathbf{U}}{\partial \mathbf{W}} \right]^{-1}. \quad (5)$$

If \mathbf{L}_A and \mathbf{R}_A are normalized so that $\mathbf{L}_A \cdot \mathbf{R}_A = \mathbf{I}$, the \mathbf{R}_U and \mathbf{L}_U will also be properly normalized.

The matrix \mathbf{A} has seven eigenvalues. Six of them correspond to the backward and forward propagating fast, intermediate, and slow waves, while the seventh is the entropy wave. Listed in order from fastest to slowest, the wave speeds are

$$\begin{aligned} \lambda_{f\pm} &= u_x \pm v_f \\ \lambda_{a\pm} &= u_x \pm v_{ax} \\ \lambda_{s\pm} &= u_x \pm v_s \\ \lambda_0 &= u_x, \end{aligned} \quad (6)$$

where

$$\begin{aligned} v_{ax}^2 &= B_x^2/4\pi\rho \\ c_s^2 &= \gamma p/\rho \\ v_a^2 &= (B_x^2 + B_\perp^2)/4\pi\rho \\ v_f^2 &= \frac{1}{2} [(v_a^2 + c_s^2) + ((v_a^2 + c_s^2)^2 - 4v_{ax}^2 c_s^2)^{1/2}] \\ v_s^2 &= \frac{1}{2} [(v_a^2 + c_s^2) - ((v_a^2 + c_s^2)^2 - 4v_{ax}^2 c_s^2)^{1/2}]. \end{aligned} \quad (7)$$

After some algebra and utilizing the normalization suggested in Brio and Wu [10], the corresponding right eigenvectors of \mathbf{A} are

$$\mathbf{r}_0 = \begin{bmatrix} \tau \\ 0 \\ 0 \\ 0 \\ 0 \\ 0 \\ 0 \end{bmatrix}, \quad \mathbf{r}_{\pm v_{ax}} = \frac{v_f}{\sqrt{2}} \begin{bmatrix} 0 \\ 0 \\ \pm \beta_z \\ \mp \beta_y \\ -\text{sgn}(B_x) \sqrt{4\pi\rho} \beta_z \\ \text{sgn}(B_x) \sqrt{4\pi\rho} \beta_y \\ 0 \end{bmatrix} \quad (8a)$$

and

$$\mathbf{r}_{\pm v_f} = \mathbf{R}_{\pm v_f} \begin{bmatrix} \mp \alpha_f \tau \\ \alpha_f v_f \\ -\alpha_s \beta_y v_{ax} \text{sgn}(B_x) \\ -\alpha_s \beta_z v_{ax} \text{sgn}(B_x) \\ \pm \alpha_s \beta_y v_f \sqrt{4\pi\rho} \\ \pm \alpha_s \beta_z v_f \sqrt{4\pi\rho} \\ \pm \alpha_f \gamma p \end{bmatrix},$$

$$\mathbf{r}_{\pm v_s} = R_{\pm v_s} \begin{bmatrix} \mp \alpha_s \tau \\ \alpha_s v_s \\ \alpha_f \beta_y c_s \operatorname{sgn}(B_x) \\ \alpha_f \beta_z c_s \operatorname{sgn}(B_x) \\ \mp \alpha_f \beta_y \frac{c_s^2}{v_f} \sqrt{4\pi\rho} \\ \mp \alpha_f \beta_z \frac{c_s^2}{v_f} \sqrt{4\pi\rho} \\ \pm \alpha_s \gamma p \end{bmatrix} \quad (8b)$$

while the left eigenvectors are

$$\mathbf{l}_0 = \left[\rho, 0, 0, 0, 0, \frac{1}{\gamma p} \right] \quad (9a)$$

$$\mathbf{l}_{\pm v_{ax}} = \frac{1}{\sqrt{2} v_f} \left[0, 0, \pm \beta_z, \mp \beta_y, -\operatorname{sgn}(B_x) \frac{\beta_z}{\sqrt{4\pi\rho}}, \operatorname{sgn}(B_x) \frac{\beta_y}{\sqrt{4\pi\rho}}, 0 \right] \quad (9b)$$

$$\mathbf{l}_{\pm v_f} = \frac{R_{\pm v_f}}{v_f^2} \left[0, \alpha_f v_f, -\alpha_s \beta_y v_{ax} \operatorname{sgn}(B_x), -\alpha_s \beta_z v_{ax} \operatorname{sgn}(B_x), \pm \frac{\alpha_s \beta_y v_f}{\sqrt{4\pi\rho}}, \pm \frac{\alpha_s \beta_z v_f}{\sqrt{4\pi\rho}}, \pm \alpha_f \tau \right] \quad (9c)$$

$$\mathbf{l}_{\pm v_s} = \frac{R_{\pm v_s}}{v_f^2} \left[0, \alpha_s v_s, \alpha_f \beta_y c_s \operatorname{sgn}(B_x), \alpha_f \beta_z c_s \operatorname{sgn}(B_x), \mp \frac{\alpha_f \beta_y c_s^2}{\sqrt{4\pi\rho} v_f}, \mp \frac{\alpha_f \beta_z c_s^2}{\sqrt{4\pi\rho} v_f}, \pm \alpha_s \gamma p \right]. \quad (9d)$$

Here, following Brio and Wu, we have used

$$\alpha_f = \frac{\sqrt{v_f^2 - v_{ax}^2}}{\sqrt{v_f^2 - v_s^2}}, \quad \beta_y = \frac{B_y}{\sqrt{B_y^2 + B_z^2}},$$

$$\alpha_s = \frac{\sqrt{v_f^2 - c_s^2}}{\sqrt{v_f^2 - v_s^2}}, \quad \beta_z = \frac{B_z}{\sqrt{B_y^2 + B_z^2}}$$

and

$$R_{\pm v_f} = \frac{v_f}{\sqrt{\alpha_f^2 (v_f^2 + c_s^2) + \alpha_s^2 (v_f^2 + v_{ax}^2)}}$$

$$R_{\pm v_s} = \frac{v_f^2}{\sqrt{\alpha_f^2 c_s^2 (v_f^2 + c_s^2) + \alpha_s^2 v_f^2 (v_s^2 + c_s^2)}}$$

The + sign refers to forward propagating waves, the – sign refers to backward propagating waves, and the normalizations $R_{\pm v_s}$, $R_{\pm v_f}$ have been chosen so that

$$\mathbf{l}_{\pm v_f} \cdot \mathbf{r}_{\pm v_f} = \mathbf{l}_{\pm v_s} \cdot \mathbf{r}_{\pm v_s} = 1.$$

With this normalization, the eigenvectors remained defined both in the limit that $B_x \rightarrow 0$, and that $B_\perp \rightarrow 0$. In the case $v_s = v_f$, when both α_f and α_s appear to be undefined, we use the limiting values $\alpha_f = \alpha_s = 1$.

3. THE SOLUTION OF THE MHD RIEMANN PROBLEM

We seek solutions to the system of MHD conservation laws

$$\frac{\partial \mathbf{U}}{\partial t} + \nabla \cdot \mathbf{F} = 0, \quad (10)$$

where \mathbf{U} is a vector of length 7 and \mathbf{F} is the flux. A Godunov code requires the flux $\mathbf{F}^G(\mathbf{U}_R, \mathbf{U}_L)$ evaluated along the ray $x/t=0$ in the Riemann problem solution to Eq. (10) with left state \mathbf{U}_L and right state \mathbf{U}_R . Since we do not need the entire solution to the Riemann problem—indeed, for non-strictly hyperbolic systems, it may not always be possible to construct the full solution—it is sufficient to develop the flux as a series of approximations to the solution along the ray $x/t=0$. In this section, we discuss our approximations to the Godunov flux and comment on how we will extend our approximation to multidimensional problems and general coordinate systems.

As we mentioned in Section 2, the MHD eigenvectors have a reasonably compact form when represented in \mathbf{W} -space. Consequently, we choose to develop the Godunov flux by working in this “primitive” variable space, \mathbf{W} . We have adopted without modification the BCT formulation for the construction of \mathbf{W}_L and \mathbf{W}_R , using the eigenvectors and eigenvalues at cell center. In the following discussion, we take \mathbf{W}_R and \mathbf{W}_L as given states in a Riemann problem.

We begin by expanding the jump $\mathbf{W}_R - \mathbf{W}_L$ in terms of a set of linearly independent vectors $\bar{\mathbf{R}}_k$, i.e.,

$$\mathbf{W}_R - \mathbf{W}_L = \sum_{k=1}^7 \bar{\alpha}_k \bar{\mathbf{R}}_k. \quad (11)$$

To determine $\bar{\mathbf{R}}_k$, define $\mathbf{W}_e = 1/2(\mathbf{W}_L + \mathbf{W}_R)$, and let $\bar{\mathbf{R}}_k = \mathbf{r}_k(\mathbf{W}_e)$ be the k th right eigenvector of $D\mathbf{F}$ at \mathbf{W}_e .

We next construct the intermediate states \mathbf{W}_L^* and \mathbf{W}_R^* as the two states which “bound” the entropy wave. That is,

$$\mathbf{W}_L^* = \mathbf{W}_L + \sum_{\lambda^-} \bar{\alpha}_k \bar{\mathbf{R}}_k$$

$$\mathbf{W}_R^* = \mathbf{W}_R - \sum_{\lambda^+} \bar{\alpha}_k \bar{\mathbf{R}}_k. \quad (12)$$

Here, λ^- refers to waves which move to the left with respect to the entropy wave, while λ^+ waves move to the right. At these two states, we evaluate the eigenvalues $\lambda(\mathbf{W}_L^*)$ and $\lambda(\mathbf{W}_R^*)$ and define the mean entropy wave speed to be

$$\bar{\lambda}_0^* \equiv \frac{1}{2}(\lambda_{0,L}^* + \lambda_{0,R}^*).$$

We approximate the wave speed λ_k for λ^- waves ($\mathbf{W}_L, \mathbf{W}_L^*$) and for λ^+ waves from ($\mathbf{W}_R, \mathbf{W}_R^*$) with a cubic Hermite interpolating polynomial. For example, for a λ^- wave from \mathbf{W}_L to \mathbf{W}_L^* , we write

$$\begin{aligned} \lambda(t) &= t\lambda_k(\mathbf{W}_L^*) + (1-t)\lambda_k(\mathbf{W}_L) \\ &+ \bar{\alpha}_k t(1-t)[(\kappa_{kk}(\mathbf{W}_L) - D)(1-t) \\ &- (\kappa_{kk}(\mathbf{W}_L^*) - D)t], \end{aligned} \tag{13}$$

where $t \in [0, 1]$, $D = (\lambda_k(\mathbf{W}_L) - \lambda_k(\mathbf{W}_L^*)) / \bar{\alpha}_k$ and κ_{kk} is the structure coefficient. The structure coefficient is defined as

$$\kappa_{kk} = (\nabla \lambda_k) \cdot \mathbf{r}_k. \tag{14}$$

This Hermite polynomial is replaced by a set of piecewise linear segments which pass through its extrema.

The mean entropy wave speed provides an unambiguous determination of the upwind state. If $\bar{\lambda}_0^* > 0$, then we choose an upwind state on the left-hand side of the entropy wave, i.e., from between the states \mathbf{W}_L and \mathbf{W}_L^* . Similarly, if $\bar{\lambda}_0^* < 0$, then we take the upwind state to be between \mathbf{W}_R and \mathbf{W}_R^* . If $\bar{\lambda}_0^* = 0$, we take the reference state to be $1/2(\mathbf{W}_R^* + \mathbf{W}_L^*)$.

Suppose for the sake of example that $\bar{\lambda}_0^* > 0$. We define the flux contributed by each wave to be

$$\mathbf{F}_k = \sum_{s=1}^{S(k)} \mathbf{F}(\mathbf{W}_k^s) (-1)^s, \tag{15}$$

where

$$\mathbf{W}_k = \mathbf{W}_L + \sum_{k' < k} \bar{\alpha}_{k'} \bar{\mathbf{R}}_{k'}, \quad k < 1, 2, 3, \tag{16}$$

and

$$\mathbf{W}_k^s = \mathbf{W}_k + \alpha_k^s \bar{\mathbf{R}}_k. \tag{17}$$

Here, α_k^s satisfies

$$\begin{aligned} \bar{\lambda}_k(\alpha_k^s) &= 0, & 2 \leq s \leq S(k) - 1, \\ \bar{\lambda}_k(\alpha_k^s) &\leq 0, & \alpha_k^1 = 0, \\ \bar{\lambda}(\alpha_k^{S(k)}) &\leq 0, & \alpha_k^{S(k)} = \bar{\alpha}_k. \end{aligned} \tag{18}$$

Summed over all the λ^- waves, the Godunov flux is

$$\begin{aligned} \mathbf{F}^G(\mathbf{W}_L, \mathbf{W}_R) \\ = \mathbf{F}(\mathbf{W}_L) + \sum_{k=1}^3 \sum_{s=1}^{S(k)} \mathbf{F}(\mathbf{W}_k^s) (-1)^s. \end{aligned} \tag{19}$$

The advantage of our method of evaluating the flux is that different subpieces of the flux can be treated differently. For example, suppose that $\mathbf{F} = \mathbf{Q}_1 + \mathbf{Q}_2$, where \mathbf{Q}_1 should be differenced as a divergence and \mathbf{Q}_2 should be differenced as a gradient. A split such as this is appropriate in the spatially varying geometry of a multidimensional simulation in non-Cartesian coordinates. Then

$$\mathbf{Q}_i^G = \mathbf{Q}_i(\mathbf{U}_L) + \sum_{k=1}^K \sum_{s=0}^S \mathbf{Q}_i(\mathbf{U}_k) (-1)^s. \tag{20}$$

4. NUMERICAL RESULTS

We have combined the flux formulation above with the higher-order considerations discussed in BCT to produce a higher-order Godunov method for the equations of MHD. We tested our higher-order method on a variety of one-dimensional problems. Here, we describe the results for two of them.

Brio and Wu [10] have proposed a test problem which extends the Sod [12] shock tube problem to MHD. The initial conditions for this problem are

$$\mathbf{W}_L(x < 0) = \begin{bmatrix} 1 \\ 0 \\ 0 \\ 0 \\ \sqrt{4\pi} \\ 0 \\ 1 \end{bmatrix}, \quad \mathbf{W}_R(x > 0) = \begin{bmatrix} 8 \\ 0 \\ 0 \\ 0 \\ -\sqrt{4\pi} \\ 0 \\ 0.1 \end{bmatrix}.$$

The other two parameters are the adiabatic index $\gamma = 2$ and $B_x = 0.75 \times \sqrt{4\pi}$.

These initial conditions correspond to a jump discontinuity in the fluid variables combined with a current sheet at $x = 0$. Unlike the Sod shock tube, which could in principle be realized in a laboratory environment, this problem is unphysical. In a real shock tube filled with plasma with these initial conditions, the magnetic field must also satisfy certain boundary conditions on the walls of the tube. These boundary conditions will influence strongly the evolution of the magnetic field and ultimately modify the nature of the entire solution. It is therefore not surprising that the results of this test problem appear nonphysical. With this caveat in mind, we still believe that the Brio and

Wu test problem is an excellent demonstration of the local linear degeneracy and lack of strict hyperbolicity in MHD.

In Fig. 1, we show the Brio and Wu problem solution at $t = 80$. In this calculation, we have used a fixed value of $\Delta t = 0.2$, a mesh spacing of $\Delta x = 1$, and a total of 800 mesh points. In the plot of the density, reading from left to right, the five waves present are a fast rarefaction wave (FR), a compound wave (SC), a contact discontinuity (CD), a slow wave shock (SS), and another fast rarefaction wave. The compound wave consists of a slow mode shock attached to

a slow mode rarefaction. These waves become degenerate and travel at the same speed when the transverse magnetic field passes through 0. These results are in excellent agreement with calculations reported by Brio and Wu. Note that the shocks appear very sharp and that there are no post-shock oscillations. There is, however, a small oscillation associated with the weak, forward-going fast wave and some wall-heating at the contact. These results were obtained with an explicit artificial viscosity of the type discussed in BCT.

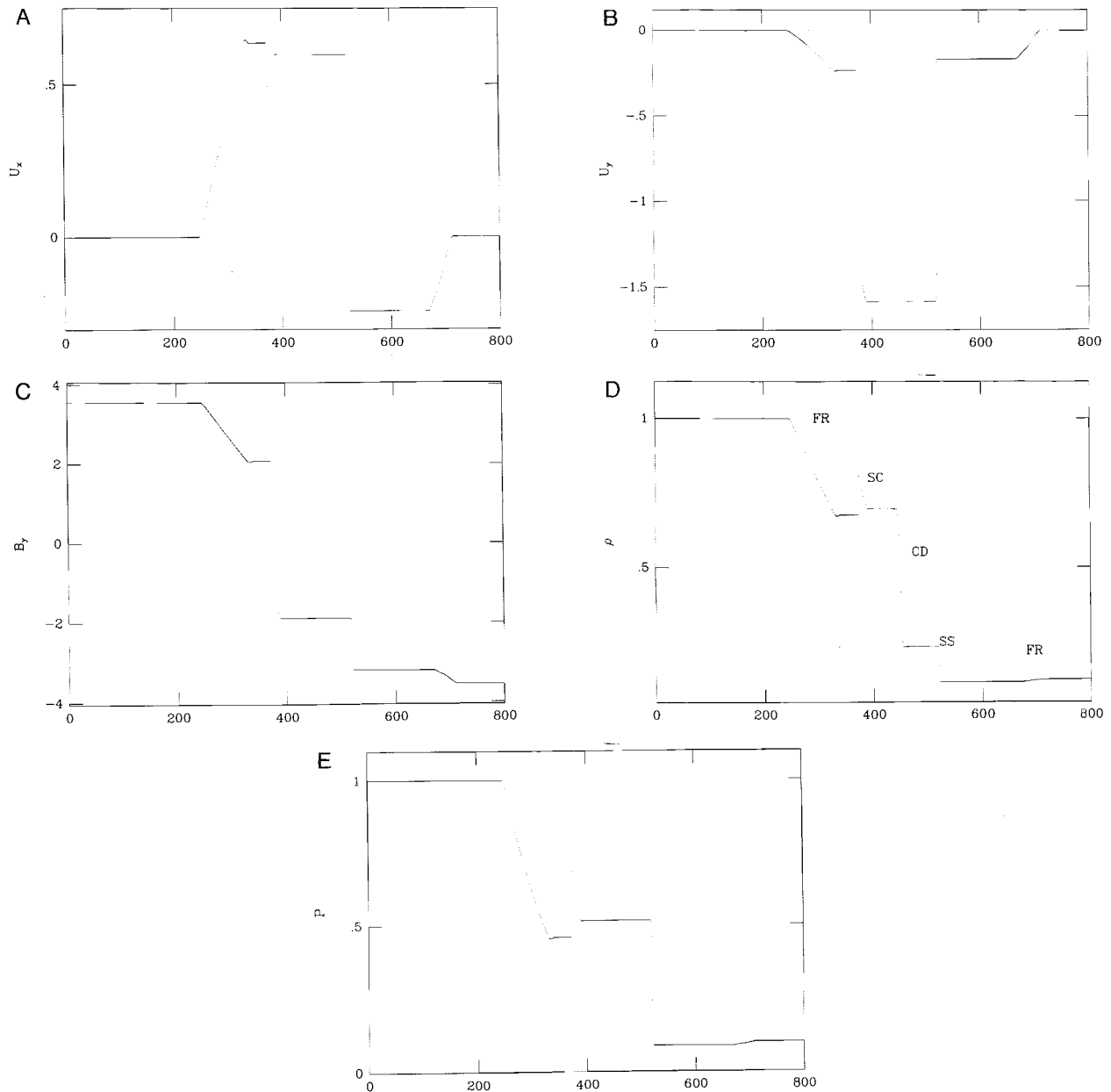


FIG. 1. The solution to the Brio and Wu version of a magnetized shock tube. The initial conditions were a jump discontinuity in pressure and density separated by a current sheet. The solution shown here is at time $t = 80$, with a fixed timestep of $\Delta t = 0.2$.

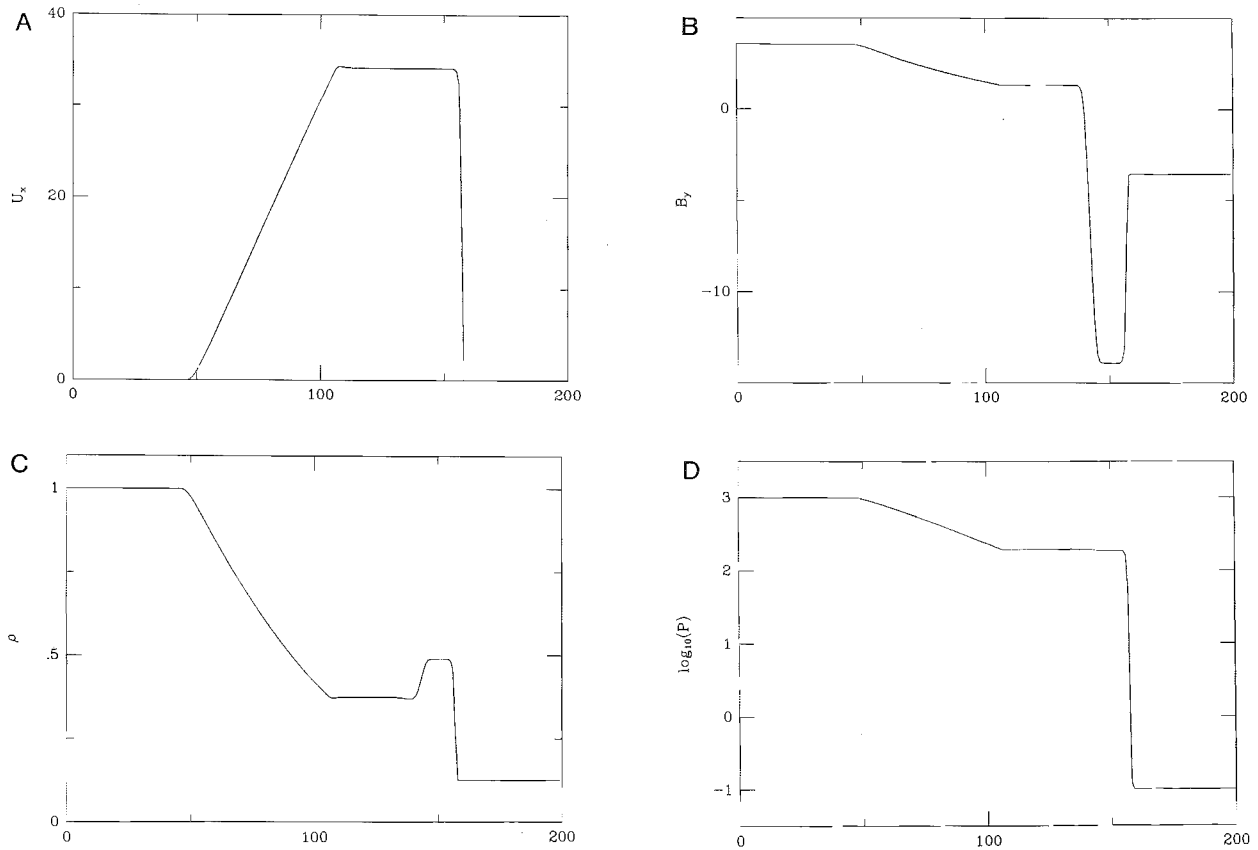


FIG. 2. The numerical solution of the second test problem, with $B_x = 0$, and B_y changing sign across the initial discontinuity. Here, we used an adiabatic index $\gamma = \frac{5}{3}$, a Courant number of 0.8, and 200 timesteps.

In the second problem, we use the initial conditions

$$\mathbf{W}_L(x < 0) = \begin{bmatrix} 1 \\ 0 \\ 0 \\ 0 \\ \sqrt{4\pi} \\ 0 \\ 1000 \end{bmatrix}, \quad \mathbf{W}_R(x > 0) = \begin{bmatrix} 8 \\ 0 \\ 0 \\ 0 \\ -\sqrt{4\pi} \\ 0 \\ 0.1 \end{bmatrix},$$

with $B_x = 0$ and $\gamma = \frac{5}{3}$. Our results, displayed in Fig. 2, show a sharp contact with some wall-heating, a fast mode shock, and are in excellent agreement with analytic calculations. These results were obtained without an explicit artificial viscosity.

5. CONCLUSIONS

We have developed a higher-order Godunov method for the equations of ideal MHD. Our algorithm is based on the methods discussed in Bell, Colella, and Trangenstein, with

appropriate extension and generalization to MHD. Our extension of the earlier definition of the flux has a natural generalization to the flux encountered in the spatially varying geometry of a multidimensional simulation. The results of some simple one-dimensional test problems show that our algorithm is sufficiently robust to deal with the lack of strict hyperbolicity as well as with the resulting degeneracy among the eigenvectors. We are in the process of constructing a multidimensional, operator split code using this methodology.

ACKNOWLEDGMENTS

We thank Arieh Königl for many stimulating discussions about MHD. The Cray XMP time at NMFEEC used to make the calculations presented here was provided by the Magnetic Fusion Energy Program and by the Office of Energy Research. This work was supported under the auspices of the United States Department of Energy by Lawrence Livermore National Laboratory under Contract W-7405-ENG-48, by NSF Grants AST 84-51727 and AST 85-03093 to the University of Chicago, and by Cray Research, Inc. Partial support was provided by the Applied Mathematical Sciences Program of the Office of Energy Research under Contract W-7405-ENG-48, and by the Air Force Office of Scientific Research under Grant AFOSR-ISSA-870016.

REFERENCES

1. P. Colella and P. R. Woodward, *J. Comput. Phys.* **54**, 174 (1984).
2. P. R. Woodward, "PPM: Piecewise-Parabolic Method for Astrophysical Fluid Dynamics," *NATO Advanced Research Workshop on Astrophysical Radiation Hydrodynamics* (Riedel, Holland, 1986).
3. R. Tamm and B. A. Fryxell, *Astrophys. J. Lett.* **327**, L73 (1988).
4. J. M. Blondin, A. Königl, and B. A. Fryxell, *Astrophys. J. Lett.* **337**, L37 (1989).
5. P. R. Woodward and P. Colella, *J. Comput. Phys.* **54**, 155 (1984).
6. D. A. Clarke, M. L. Norman, and J. O. Burns, *Astrophys. J. Lett.* **311**, L63 (1986).
7. J. B. Bell, P. Colella, and J. A. Trangenstein, *J. Comput. Phys.* **82**, 362 (1989).
8. T. P. Liu, *J. Diff. Equations* **18**, 218 (1975).
9. B. Engquist and S. Osher, *Math. Comput.* **36**, 321 (1981).
10. M. Brio and C. C. Wu, *J. Comput. Phys.* **75**, 400 (1988).
11. A. Jeffrey and T. Taniuti, *Non-linear Wave Propagation* (Academic Press, New York, 1964).
12. G. Sod, *J. Comput. Phys.* **27**, 1 (1978).

Received November 15, 1988; revised March 4, 1991

ANDREW L. ZACHARY¹

*Department of Astronomy and Astrophysics
University of Chicago
Chicago, Illinois 60637*

PHILLIP COLELLA²

*Lawrence Livermore National Laboratory
Livermore, California*

¹ Now at Cray Research, Inc., Darien, CT.

² Now at Department of Mechanical Engineering, University of California, Berkeley, CA.